the plant journal

SEB SOCIETY FOR EXPERIMENTAL BIOLOGY

The Plant Journal (2019) doi: 10.1111/tpj.14511

AtHB23 participates in the gene regulatory network controlling root branching, and reveals differences between secondary and tertiary roots

María F. Perotti, Pamela A. Ribone†, Julieta V. Cabello†, Federico D. Ariel* and Raquel L. Chan*

Instituto de Agrobiotecnología del Litoral, Universidad Nacional del Litoral, CONICET, FBCB, Centro Científico Tecnológico CONICET Santa Fe, Colectora Ruta Nacional No 168 km. 0, Paraje El Pozo, 3000, Santa Fe, Argentina

Received 7 May 2019; revised 2 August 2019; accepted 19 August 2019.
*For correspondence (e-mail fariel@santafe-conicet.gov.ar; rchan@fbcb.unl.edu.ar).
†These authors equally contributed to this manuscript.

SUMMARY

In Arabidopsis, lateral root (LR) development is mainly controlled by several known auxin-regulated transcription factors (TFs). Here, we show that AtHB23 (a homeodomain-leucine zipper I TF) participates in this intricate network. Our study of the expression pattern of *AtHB23* revealed that it is transcriptionally activated in the early stages of secondary LR primordium (LRP). We found that AtHB23 directly limits the expression of *LBD16*, a key factor in LR initiation, and also directly induces the auxin transporter gene *LAX3*. We propose that this HD-Zip I mediates the regulation of *LAX3* by ARF7/19. Furthermore, AtHB23 plays distinct roles during the formation of secondary and tertiary roots, exhibiting differential expression patterns. *ATHB23* is expressed throughout the tertiary root primordium, whereas it is restricted to early stages in secondary primordia, likely later repressing *LBD16* in tertiary LR development and further inhibiting root emergence. Our results suggest that different genetic programs govern the formation of LRP from the main or secondary roots, thereby shaping the global dynamic architecture of the root system.

Keywords: lateral roots, tertiary roots, AtHB23, LBD16, LAX3, ARF7/19.

INTRODUCTION

The root system depends on the main root length, together with the number and density of lateral roots (LRs), which develop from auxin-dependent *de novo* meristems. LR development mimics the organogenesis of the primary root in terms of tissue composition and organization. Notably, this process can be reiterated in subsequent higher-order LRs (Osmont *et al.*, 2007). Little is known about the formation of tertiary roots, for example, LRs formed from emerged secondary roots, which ultimately contribute to the three-dimensional architecture of the root system. Knowledge about the mechanisms governing LR development has considerably increased in recent years, particularly in the model plant Arabidopsis, and research has revealed the role of auxin as an integrator of many internal and external signals that modulate LR formation (Lavenus *et al.*, 2013).

Lateral roots initiate at regular intervals along the primary roots from founder cells, principally in the pericycle (De Smet *et al.*, 2007; Lucas *et al.*, 2008), and undergo asymmetric divisions. Fine coordination between cell cycle activation and cell polarity/identity specification processes, involving auxin, is needed for LR initiation. Auxin integrates a wide range of intrinsic and environmental signals to modulate LR development, based on the spatial expression diversity of auxin receptors (Calderón Villalobos *et al.*, 2012).

In roots, auxin is transported toward the tip through the central cylinder (Friml *et al.*, 2003). In Arabidopsis, auxin influx carriers, encoded by *AUX1*, *LAX1*, *LAX2* and *LAX3* genes, exhibit differential expression patterns and roles (Péret *et al.*, 2012; Swarup and Péret, 2012). AUX1 has been described as a regulator of LR initiation and LAX3 induces LR emergence, whereas LAX2 is involved in vascular patterning in cotyledons (Marchant *et al.*, 1999, 2002; De Smet *et al.*, 2007). LAX1 and LAX2 are together required for leaf phyllotactic patterning (Péret *et al.*, 2012), and LAX2 has also been linked to the regulation of xylem development and lateral-vein symmetry (Moreno Piovano *et al.*, 2017).

Root development involves transcription factors (TFs) from different families in an intricate network (Lavenus *et al.*, 2015). Among these, lateral organ boundaries (LBDs) and auxin response factors (ARFs) TFs are the main actors. LBD16 and LBD29 have been associated with the acquisition

of LR founder cell polarity and cell cycle activation (Okushima *et al.*, 2007; Lee *et al.*, 2009; Goh *et al.*, 2012). LBD18 and LBD33 have also been associated with cell cycle activation (Lee *et al.*, 2009; Berckmans *et al.*, 2011), whereas LBD18 has been assigned a role in the upregulation of cell wall remodeling genes (Lee *et al.*, 2012). LBD16 and LBD29 are expressed in pericycle cells prior to LR initiation, and researchers have proposed that these TFs have different sets of targets (Porco *et al.*, 2016). LBD14 was recently linked to LR formation in response to abscisic acid (ABA; Jeon *et al.*, 2017). ARF- and LBD-encoding genes act in modules (Lavenus *et al.*, 2013). For example, in LR founder cells, *LBD16* and *LBD29* are targets of the module indole acetic acid (IAA)14–ARF7/ARF19, whereas in the cortex and epidermis, the same module regulates *LBD18* (Lee *et al.*, 2012) and the auxin transporter *LAX3* (Swarup *et al.*, 2008; Kumpf *et al.*, 2013). ARF7 and ARF19 activate early auxin-responsive genes, as shown by the double *arf7/arf19* mutant being impaired in LR development. The overexpression of their targets, *LBD16* and *LBD29*, induces LR formation, even in the absence of ARF7 and ARF19 (Okushima *et al.*, 2007). It was recently shown that the direct recognition of *LBD16* by ARF7 in response to water availability is modulated by ARF7 SUMOylation, which modulates root hydropatterning (Orosa-Puente *et al.*, 2018).

HD-Zip TFs belong to the superfamily of homeodomain (HD)-containing proteins (Chan *et al.*, 1998), first discovered in animals from the homeotic effect resulting from their mutation or ectopic expression (Gehring, 1987). The association between the HD and the leucine zipper (LZ) dimerization motif is unique to plants, and HD-Zip proteins have been classified in four groups, I–IV, according to their structure and the presence of additional motifs (revised in Ariel *et al.*, 2007). HD-Zip I members have been associated with the responses to stress and different developmental events (for review, see Perotti *et al.*, 2017). In the model legume *Medicago truncatula*, the HD-Zip I member MtHB1 was reported to be a regulator of LR emergence in response to stress, via the direct repression of the LBD TF *MtLBD1* (Ariel *et al.*, 2010a,b).

AtHB23 is a member of subfamily I of HD-Zip TFs and, according to structural features resolved in phylogenetic trees, has a paralog, AtHB13 (Henriksson *et al.*, 2005; Arce *et al.*, 2011). However, these TFs exhibit independent functions and different expression patterns. *AtHB23* has been described as being expressed in the adaxial region of leaves (Kim *et al.*, 2007), and also as being involved in hypocotyl elongation and cotyledon expansion under red light (Choi *et al.*, 2014). *AtHB13* has a role in abiotic and biotic stress responses, pollen hydration and seed germination (Hanson *et al.*, 2001, 2002; Cabello and Chan, 2012; Gao *et al.*, 2014; Ribone *et al.*, 2015; Silva *et al.*, 2016). Both *AtHB13* and *AtHB23* are involved in the inhibition of inflorescence stem elongation, which drives cell proliferation, although their roles are not redundant (Ribone *et al.*, 2015). The roles of AtHB13 and AtHB23 in root development remain unexplored.

The ability of roots to branch contributes substantially to their capacity to explore the soil for water and nutrients, which has allowed plants to successfully colonize land (Motte and Beeckman, 2019). Extensive work has been devoted to uncovering the mechanisms underlying LR development, for example, the initiation, primordium formation and emergence from primary roots. Notably, hormone and salt stress signaling differ significantly between LRs and the primary root. Salinity stress activates high levels of ABA signaling exclusively in LR growth, and the primary root is less sensitive to salt treatment compared with LRs (Duan *et al.*, 2013). It is well known that LR initiation is dependent on auxin accumulation and, once the new organ protrudes from the main root, the novel meristem can produce auxin (Lijung *et al.*, 2005), but at which precise stage such ability occurs remains unclear. Remarkably, the molecular and physiological mechanisms governing LR development from secondary roots (tertiary roots) remain unexplored, but it is likely assumed that LR formation is governed by the same genetic program, whether initiated from the main or a secondary root.

In this work, we investigate the role of AtHB23 in root development. *AtHB23* is expressed at the base of the secondary LR primordium (LRP); we show by chromatin immunoprecipitation-quantitative polymerase chain reaction assays (ChIP-qPCR) that this TF directly controls *LBD16*. Furthermore, AtHB23 can directly regulate the auxin transporter gene *LAX3*. Remarkably, *LAX3* promoter activity in secondary roots is dependent on AtHB23. *AtHB23*-silenced (*artificial miR23*, *35S:amiR23*) plants exhibited more initiated LR than wild-type (WT) plants. Furthermore, we discovered that *AtHB23* is differentially expressed during LR initiation and emergence, depending on if the primordium is formed from the main or a secondary root. Accordingly, *amiR23* plants exhibited more initiated and emerged tertiary roots. Altogether, our results indicate that ATHB23 participates in different molecular mechanisms that drive LR formation in the main or secondary roots by the direct regulation of auxin-related genes. Our work expands our understanding of the complex regulatory and dynamic network orchestrating LR development from primary or secondary roots.

RESULTS

AtHB23 represses the initiation of secondary roots

The analysis of the *AtHB23* promoter region that drives the expression of the *GUS* reporter gene first indicated this role of this TF in LR development. Along the main root, *AtHB23* promoter activity was detected in zones surrounding the first divisions of LR development (Figure 1a). Until

LR developmental stage IV (Malamy and Benfey, 1997), the activity of the *AtHB23* promoter is restricted to the base of the LRP (defined according to Malamy and Benfey, 1997). However, from stage IV until emergence, no expression was detected in the newly formed LR. Later, GUS staining was clearly visible in the vascular system of the secondary root, but not visible in the main root (Figure 1b, and additional independent transgenic lines in Figure S1a). Histological sections, taken from the primary root, showed that *AtHB23* expression is limited to the base of the LRP (Figure 1c). The promoter activity of *AtHB23* revealed the transient phase of expression of this gene in early-stage primordia, for example, from stages II to IV, hinting at the role of AtHB23 in the initiation of LR.

In order to investigate the role of *AtHB23* in LR formation, we obtained silenced and overexpressor plants transformed with *35S:amiR-AtHB23* (an artificial-miRNA against *AtHB23* 3′-UTR, completely different from its closest homolog gene *AtHB13*, or *amiR23*). We chose three independent lines that we consistently characterized throughout this work (*amiR23-1* in the main figures, and *amiR23-2 and -3* in the associated supplementary figures). Additionally, we used independent *35S:AtHB23* lines (called hereafter *AT23*). *AtHB23* transcript levels were assessed in three independent lines of both transgenic genotypes compared with Col 0 (Figure S2). Primary root length and the density of initiated and emerged roots were quantified. No significant differences were detected between genotypes for the 8-day-old main root length or the density of emerged LRs assessed in the three independent lines (Figures 1d,f and S3a,c). However, the density of initiated LRs was significantly higher for *amiR23*-silenced plants than for the control Col 0 or the overexpressor *AT23* (Figures 1e and S3b), which influenced the total number of LRs (Figures 1g and S3d). Interestingly, a detailed characterization of LRPs in each genotype revealed that the higher density of initiated LRs in *amiR23* plants corresponds to an increased proportion of initiated roots at stage IV compared with Col 0 and overexpressor plants (Figure 1h). Moreover, the differential phenotype of *amiR23* plants was rescued when transformed with the construct *35S:AtHB23* (Figure S4). The results indicate that *AtHB23* participates in LR initiation.

AtHB23 is an auxin-responsive gene, and *amiR23*-silenced plants exhibit altered sensitivity to exogenous auxin

Considering the integrating role of auxin in LR development, we wondered whether it may regulate *AtHB23*

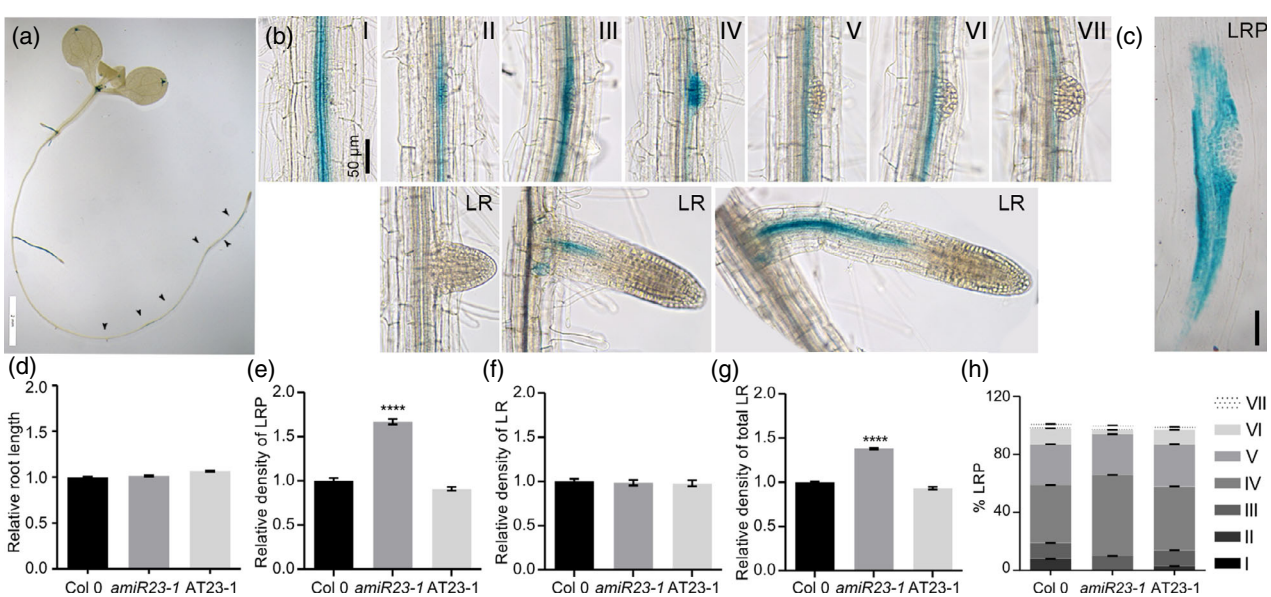

Figure 1. *AtHB23* is expressed in the secondary root initiation zone and acts as a repressor of lateral root initiation.
(a) GUS expression driven by *AtHB23* promoter in the main root of 8-day-old seedlings. Arrows indicate lateral root (LR) initiation zone.
(b) I–VII represent different stages of lateral root primordium (LRP) and LR indicates emerged roots as described by Malamy and Benfey (1997). Black bar represents 50 µm.
(c) Histological longitudinal cut of the main root after GUS histochemistry.
(d) Relative primary root length of 8-day-old Col 0, *amiR23-1* and *AT23-1* plants (*AtHB23*-silenced and overexpressor plants, respectively).
(e, f) Relative density of LRP or LR, calculated as the number of LRP or LR/mm of main primary root.
(g) Relative density of total lateral roots (LRP + LR).
(d–h) The values were normalized with those measured in the Col 0 control, taken as 1 (one); absolute values for reference were 1 = 30.44 mm (d); 1 = 0.33 LRP/mm (e); 1 = 0.17 LR/mm (f); 1 = 0.50 total LR/mm (g).
(h) Proportion of LRP in each developmental stage as defined by Malamy and Benfey (1997). The assays were repeated at least three times with *N*: 15/genotype. Error bars represent SEM. Asterisks indicate significant differences doing a Student's *t*-test between Col 0 and each transgenic line (**$P < 0.01$, ***$P < 0.001$, ****$P < 0.0001$).

expression. Thus, we treated 7-day-old seedlings with exogenous 1 μM IAA, and showed that *AtHB23* transcript levels significantly decrease after 3 h and peak at 12 h (Figure 2a). The 12-h induction was further corroborated by analysis of transgenic plants carrying the *AtHB23* promoter that drives *GUS* expression (Figure 2b). Furthermore, we assessed the effect of auxin treatment on *amiR23*, *AT23* and Col 0 seedlings. The formation of LRP responded differently to auxin in *amiR23* plants. This is because the three genotypes (*amiR23*, *AT23* and WT) had similar numbers of LRP after the treatment, indicating that auxin can compensate for *AtHB23* knockdown (Figures 2c–f and S5). Additionally, the significant difference in LR density between *amiR23* mutants and Col 0 disappeared in the presence of NPA (an inhibitor of auxin efflux; Teale and Palme, 2018; Figure S6), thus linking the role of AtHB23 with the presence of auxin in the plant roots.

Auxin influx/efflux carriers' transcripts and auxin distribution are altered in *amiR23* plants

Considering the link between *AtHB23* and auxin, we decided to investigate the expression of the selected auxin carriers *LAX1*, *AUX1* and *LAX3*, and the peak of auxin response (shown by the DR5 synthetic reporter) in *amiR23* plants. The selection of such carriers was done based on their previously reported expression patterns in roots (Péret *et al.*, 2012). *AmiR23*-silenced plants were crossed with *DR5:GUS* plants (showing the peak of auxin response; Ulmasov *et al.*, 1997), as well as with plants transformed with *LAX1*, *AUX1* and *LAX3* promoters that drive the expression of *GUS*. Interestingly, the histochemical analyses of each cross under the same conditions hint at the reduction of GUS-derived products compared with the corresponding parental plants (Figure 3). Most notably, the expression pattern of the *LAX3* promoter was specifically

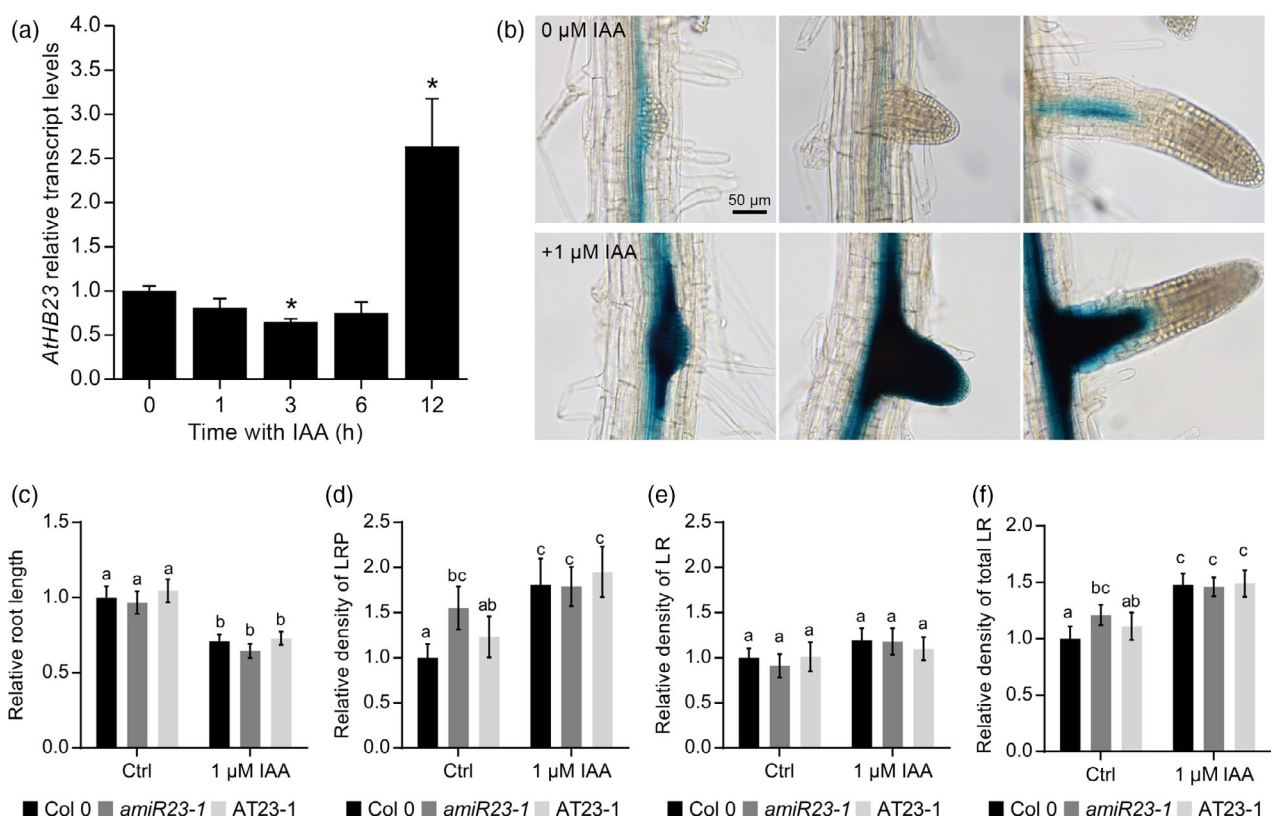

Figure 2. *AtHB23*-silenced plants are less sensitive to auxin.
(a) Transcript levels of *AtHB23* in 7-day-old roots of seedlings grown in standard conditions or with 1 μM indole acetic acid (IAA) added for 1, 3, 6 or 12 h.
(b) GUS histochemistry of 8-day-old *AtHB23:GUS* roots grown in control conditions (upper panel) or treated with 1 μM IAA (lower panel) during 12 h. Black bar indicates 50 μm.
(c) Relative primary root length of 8-day-old Col 0, *amiR23-1* and *AT23-1* plants (*AtHB23*-silenced and overexpressor plants, respectively) grown in control conditions or treated with 1 μM IAA.
(d, e) Relative density of lateral root primordium (LRP) or lateral root (LR), calculated as the number of LRP or LR/mm of main primary root, grown in control conditions or treated with 1 μM IAA.
(f) Relative density of total LR (LRP + LR), treated or not with 1 μM IAA.
(c–f) The values were normalized with those measured in the Col 0 control, taken as 1 (one); absolute values for reference were 1 = 30.99 mm (c); 1 = 0.18 LRP/mm (d); 1 = 0.21 LR/mm (e); 1 = 0.39 total LR/mm (f). The assays were repeated at least three times with *N*: 15/genotype. Error bars represent SEM. Different letters indicate significant differences (Tukey test, $P < 0.01$).

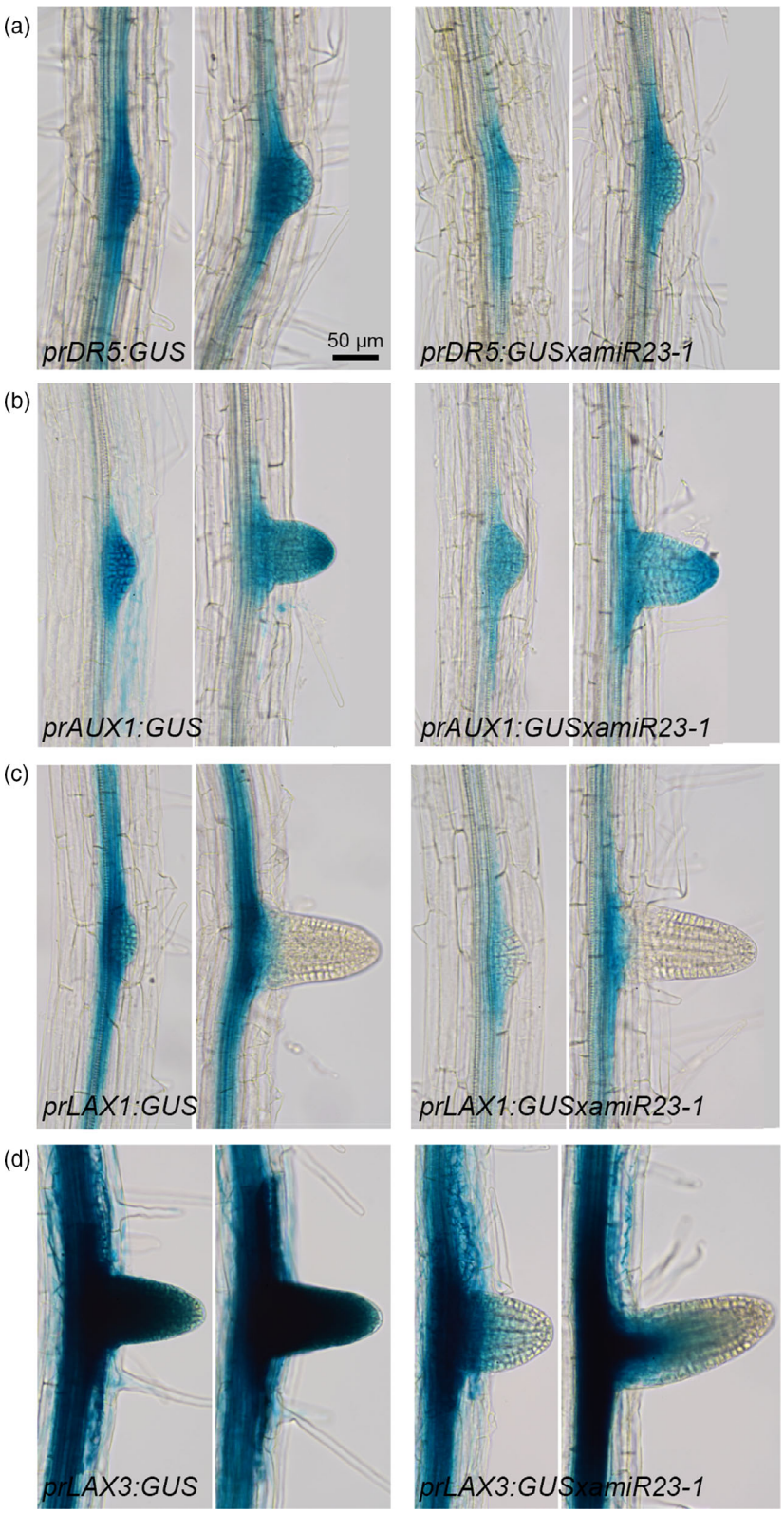

Figure 3. *LAX3* expression is repressed in *AtHB23* silenced plants.
Left panel: (a–d) overnight histochemistry of GUS in single transgenic (*DR5:GUS*, *AUX1:GUS*, *LAX1:GUS* and *LAX3:GUS*) 8-day-old plants.
Right panel: plants described in left panel crossed with the *amiR23-1* plants. Black bar represents 50 µm.

impaired, for example, it remained active in the main root, whereas GUS overnight staining was completely abolished from emerged LRs (Figure 3d). Note that GUS staining was performed overnight. Figure S7(a) shows that the GUS reaction after 3 h with *ProLAX3:GUS* exhibited a more restricted expression pattern compared with that observed

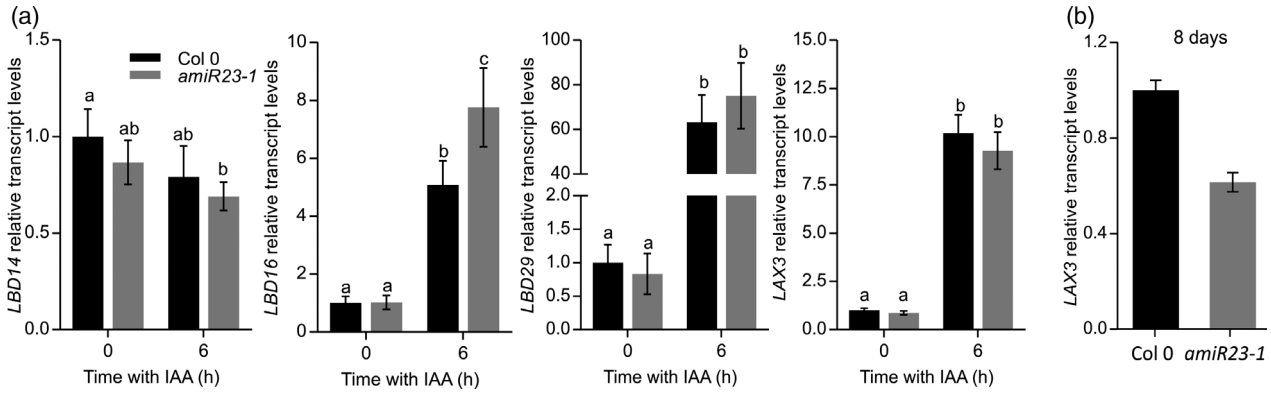

Figure 4. *LBD16* and *LAX3* are regulated by AtHB23. Expression levels of *LBD14*, *LBD16*, *LBD29* and *LAX3* in 7-day-old roots treated (or not) with 1 μM indole acetic acid (IAA).
(a) Transcript levels in Col 0 and *amiR23-1* plants.
(b) *LAX3* expression levels in 8-day-old in the same genotypes. All the values were normalized with the one obtained in Col 0 (a, b). Bars represent SEM. Data were analyzed using a two-way ANOVA considering genotype and treatment. Different letters indicate significant differences (Tukey test, $P < 0.01$).

after 12 h, in accordance with previous reports (Swarup *et al.*, 2008). The AtHB23-mediated regulation of auxin transporters seems to be specific to *LAX3*, as crossed plants bearing *LAX1* and *AUX1* promoters did not show any change in the pattern of GUS expression (Figure 3b,c). These results strongly indicate a positive and tissue-specific regulation of *LAX3* by AtHB23, as well as a slight modulation of the other two carriers and DR5 activity.

LBD16 and *LAX3* regulation depends on AtHB23

Lateral organ boundaries (*LBD*) genes were associated with events related to LR initiation and emergence. In particular, *LBD16* and *LBD29* are induced by auxin, and LBD29 regulates *LAX3* expression at the early stages of LRP (Porco *et al.*, 2016). LBD14 was recently linked to LR emergence (Jeon *et al.*, 2017). The *LBD14*, *LBD16*, *LBD29* and *LAX3* promoters were analyzed for the presence of target sequences of HD-Zip I TFs. All presented one putative perfect pseudopalindrome CAAT(A/T)ATTG, previously reported as a target sequence of HD-Zip I proteins both *in vitro* and *in vivo* (Palena *et al.*, 1999; Johannesson *et al.*, 2001; Ariel *et al.*, 2010a). To further decipher the underlying molecular mechanism mediated by AtHB23 in auxin-dependent LR development, the transcript levels of selected *LBD* genes were firstly assessed in *amiR23*-silenced roots 7 days after germination, treated or not with 1 μM IAA. *LBD16* was significantly more induced by auxin in *amiR23* plants, indicating that AtHB23 represses *LBD16* during LR formation (Figure 4a). *LBD29* and *LAX3* did not show any difference between WT (Col 0) and *amiR23* roots in response to auxin (Figure 4a,b). Furthermore, *LAX3* was repressed in *amiR23*-silenced plants later in development (8-day-old seedlings), when LR emerged (Figure 4b). Considering the different transcriptional effects of AtHB23 on *LBD16* and *LAX3*, our results indicate that this HD-Zip TF participates in alternative mechanisms that modulate auxin-responsive genes.

LBD16 and *LAX3* genes are directly regulated by AtHB23

We then wondered if AtHB23 may directly regulate key factors in LR development. Therefore, we conducted ChIP assays followed by qPCR (ChIP-qPCR) using seedlings transformed with *PromAtHB23:AtHB23:GFP:GUS* (transgene expression levels are shown in Figure S8). Then, we assessed the direct binding of AtHB23 to the perfect HD-Zip I target pseudopalindrome CAAT(A/T)ATTG present in *LBD14*, *LBD16*, *LBD29* and *LAX3* (Figure 5a). Strikingly, *LBD16* and *LAX3* promoters were recognized as direct targets of AtHB23, in contrast to *LBD14* and *LBD29* promoters. Thus, we analyzed in more detail the promoter regions of *LBD16* and *LAX3*. For *LAX3*, AtHB23 specifically bound to the perfect HD-Zip-predicted *cis*-acting element (−135 bp, P3), whereas none of the other further regions analyzed, including an imperfect HD-Zip box (P2), were retrieved (Figure 5b). Altogether, these results indicate that AtHB23 is able to directly regulate both *LBD16* and *LAX3*.

ARF7 directly controls *AtHB23*, which mediates its regulation over *LAX3*

In order to better determine the position of AtHB23 in the intricate network of TFs that coordinate LR development, the transcript levels of *AtHB23*, *LBD16* and *LAX3* were assessed in the *arf7/arf19* mutant in standard conditions or after auxin induction at 12 h (Figure 6a). The transcript levels of *AtHB23*, *LBD16* and *LAX3* were induced by auxin in Col 0, in accordance with previous reports, whereas the expression of these genes in the *arf7/arf19* mutant was insensitive to auxin treatment. In view of these results, we wondered if AtHB23 was a direct target of ARF TFs. To test this hypothesis, a ChIP assay was carried out using isolated nuclei from plants transformed with glucocorticoid receptor-tagged *PromARF7:ARF7:GR*, inducible by dexamethasone (Lavenus *et al.*, 2015). Before harvesting, plants

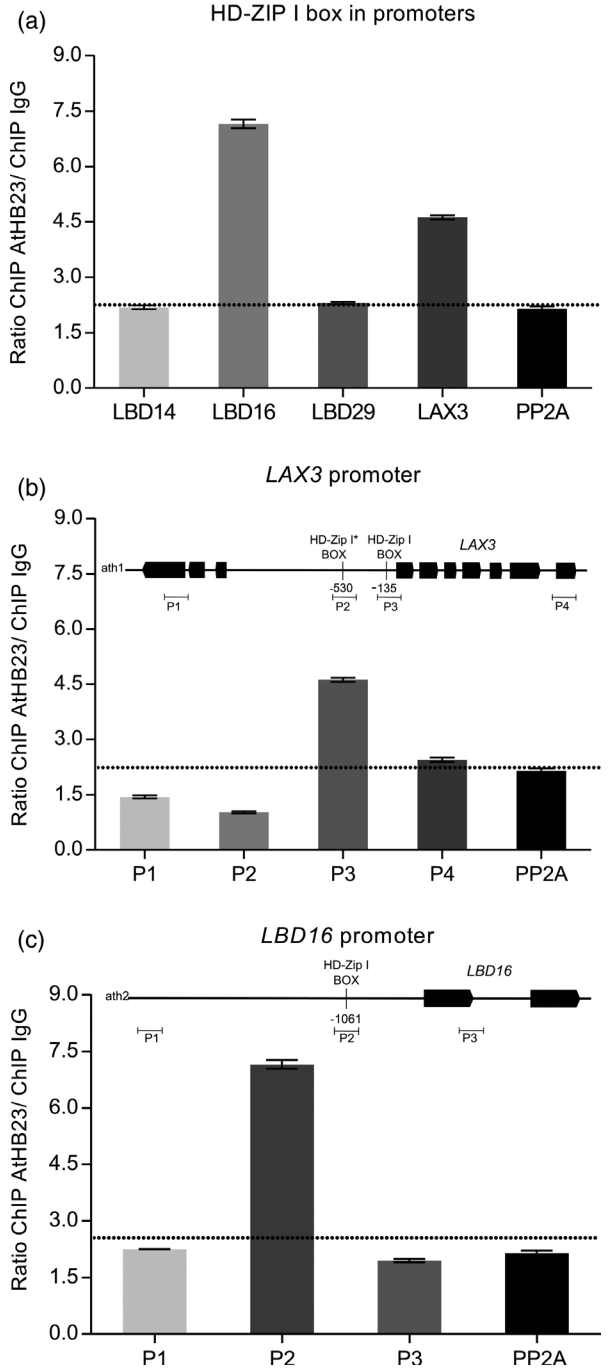

Figure 5. AtHB23 directly regulates *LBD16* and *LAX3*. Chromatin immunoprecipitation assay (ChIP-PCR) using nuclei obtained from *PromAtHB23:AtHB23:GFP:GUS* 10-day-old seedlings.

(a) The consensus HD-Zip target sequences present in the promoters of *LBD14, 16, 29* and *LAX3* were assessed for AtHB23 binding *in vivo*.

(b) Different putative regulated sequences were evaluated in *LAX3* with *PromAtHB23:AtHB23:GFP:GUS* nuclei.

(c) Putative regulated sequences evaluated in *LBD16* gene with the same seedlings. In (b, c) schematic representation of *LAX3* and *LBD16* genes indicating where the designed oligonucleotides match for each box (P1, P2, P3 and P4). *PP2A* was used as negative control, determining the background level. Values are expressed as the ratio between AtHB23:GFP IP and IgG IP used as negative control. Bars represent SE.

were treated for 4 or 12 h with 1 μM IAA to promote ARF7 activation. In the promoter region of *AtHB23*, we were able to identify two putative *cis*-acting elements described as bound by ARF TFs (Figure 6b). Remarkably, both *cis*-elements present in *AtHB23* promoter were directly bound by ARF7, with *LBD16* promoter used as a positive control (Lavenus *et al.*, 2015; Orosa-Puente *et al.*, 2018), in contrast to other regions used as negative controls (Figure 6c,d). Interestingly, *LBD16* promoter was bound with 4 h treatment but not with 12 h, in accordance with the previously reported dynamic modulation of this gene (Orosa-Puente *et al.*, 2018). In contrast, one of the *cis*-acting elements of *AtHB23* promoter was bound both with 4 and 12 h of treatment, whereas binding to the other site was only noticed at 4 h, indicating different dynamic kinetics of both ARF7 targets. Altogether, our results show that ARF7 directly controls *AtHB23* expression during LR development.

Secondary and tertiary roots exhibit different gene expression patterns and developmental programs

As shown above, the transcriptional regulation of *LAX3* by AtHB23 specifically occurs in the emerged LR, although this gene is expressed during secondary and tertiary LR development (Figure S7a,b). Therefore, we further explored how *AtHB23* is expressed in this lateral organ. Surprisingly, GUS expression driven by *AtHB23* promoter along secondary roots revealed a strong and extended activity in LRP, the so-called tertiary roots (Figure 7b,c). This staining clearly differs from the expression pattern of a secondary LRP, for example one formed from a primary root (Figures 1a,b and 7a). Furthermore, GUS expression continued to be steady and strong during the emergence of tertiary roots (Figures 7c and S1b). Note that from stage V to the emergence of the tertiary root, the *AtHB23* expression pattern is particularly different from secondary roots, in which *AtHB23* expression suddenly shut off (Figure 1b). Moreover, the secondary root remained stained upon the emergence of the tertiary root, whereas the primary root at the equivalent stage did not show GUS staining (for an easy comparison, see Figure S1). Overnight GUS staining revealed that *ProLAX3* activity is extended throughout the primordium of emerged secondary and tertiary roots (Figure S7a,b). However, *ProLAX3* is still active in the *amiR23-1* background in tertiary roots (but not in secondary roots), which suggests that *ProLAX3* activation can bypass AtHB23 only in tertiary roots (Figure S7c). Taken together, our results suggest that a differential AtHB23-mediated genetic program takes place in the formation of secondary and tertiary roots.

These observations led us to explore in more detail tertiary root development and compare it with that of secondary roots. Notably, we were unable to find in the literature any characterization of this developmental context in any dicot species.

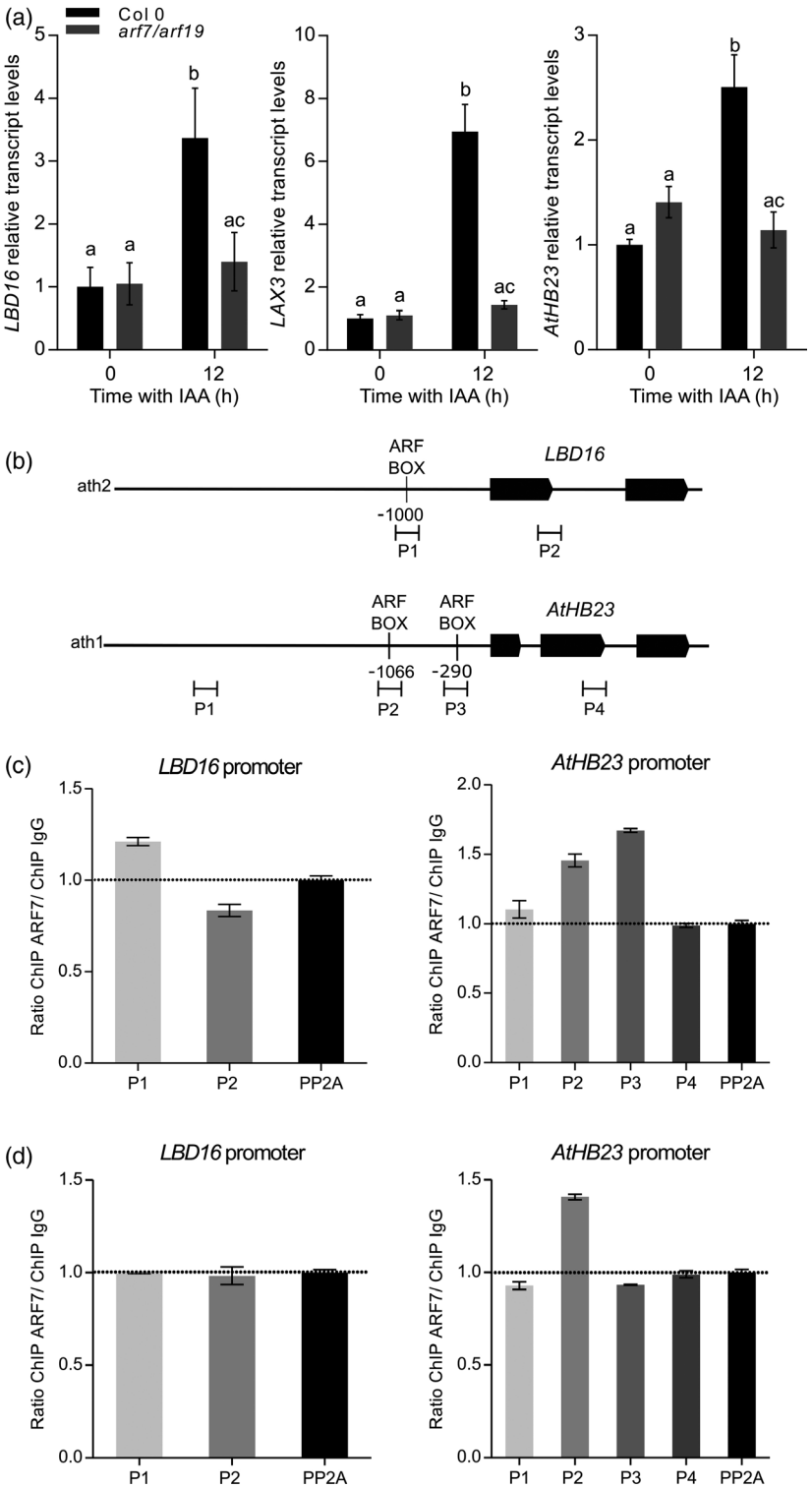

Figure 6. Transcriptional activation by auxin of *LBD16*, *LAX3* and *AtHB23* is dependent on ARF7/19.
(a) Transcript levels of *LBD16*, *LAX3* and *AtHB23* in 7-day-old Col 0 and *arf7/19* mutant roots of seedlings grown in standard conditions or with 1 μM indole acetic acid (IAA) added for 12 h. Bars represent SEM. Different letters indicate significant differences (Tukey test, $P < 0.01$).
(b) Schematic representation of *AtHB23* and *LBD16* promoters indicating where the designed oligonucleotides used in (c, d) match for each box (P1, P2 for *LBD16* and P1, P2, P3 and P4 for *AtHB23*).
(c, d) Different putative regulated sequences were evaluated in *LBD16* and *AtHB23* promoters with *PromARF7:ARF7:GR* 15-day-old seedlings treated during 4 h (c) or 12 h (d) with 1 μM IAA plus 2 μM dexamethasone. *PP2A* was used as negative control, determining the background level. Values are expressed as the ratio between ARF7:GR IP and IgG IP used as negative control. Bars represent SE.

Considering these observations, we assessed tertiary root formation in Col 0 and *amiR23*-silenced plants. Remarkably, 15 days after germination, *AtHB23* knockdown resulted in a higher density of initiated and emerged TLRs than did WT (Figures 7d and S9), indicating that AtHB23 is involved in the initiation of secondary and tertiary roots but participates also in the emergence of tertiary roots. Altogether, our results suggest that the initiation and development of tertiary and secondary roots are regulated by alternative transcriptional complexes involving AtHB23,

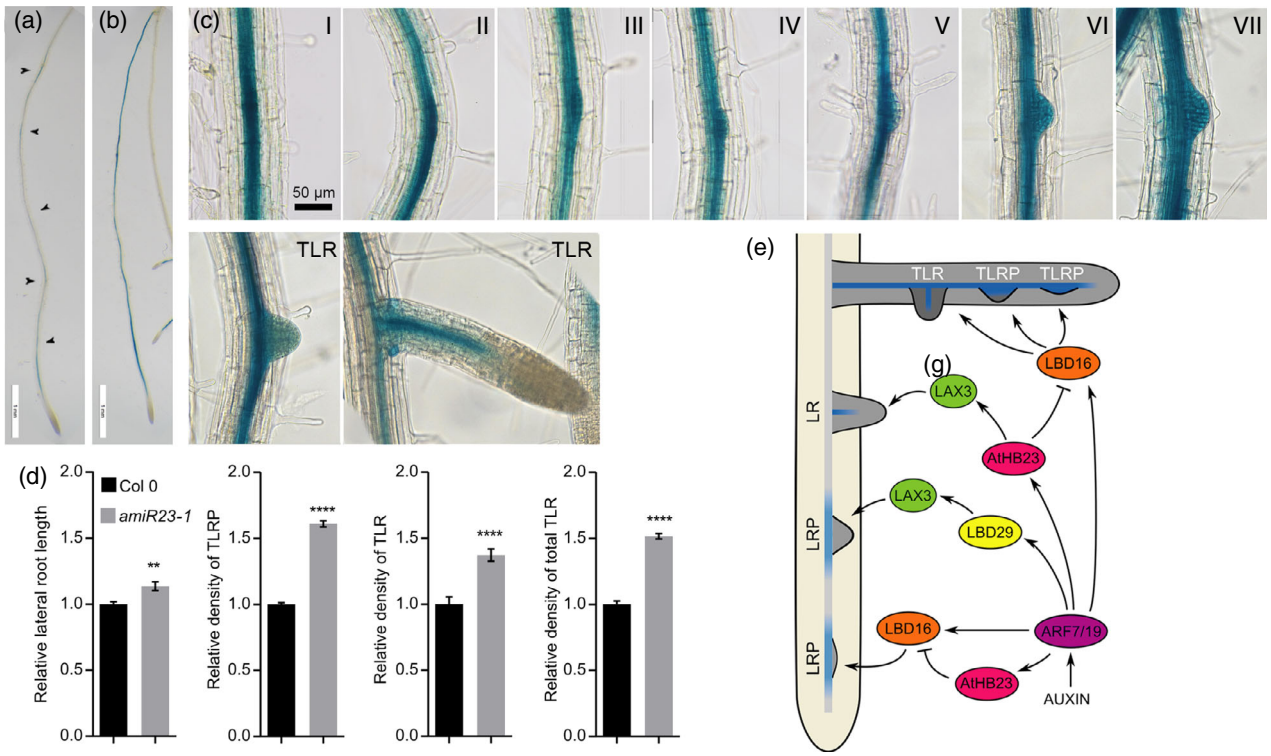

Figure 7. *AtHB23* expression pattern is different in primary and secondary roots.
AtHB23 expression in primary (a) and secondary (b) roots of 15-day-old *PromAtHB23:GUS* seedlings. Arrows indicate lateral root (LR) initiation zone.
(c) *AtHB23* expression pattern during formation of tertiary roots. I–VII represent different stages [following the classification done for lateral root primordium (LRP) by Malamy and Benfey, 1997] of tertiary lateral root primordium (TLRP) and tertiary emerged roots (TLR). Black bar represents 50 µm.
(d) Relative density of total lateral root length, TLRP, TLR and total tertiary roots (TLRP + TLR) in Col 0 and *amiR23-1* 10-day-old silenced plants. The values were normalized with those measured in the Col 0, taken as 1 (one). Absolute values for reference were in (d); 1 = 38.4 mm (root length), 1 = 0.36 TLRP/mm, 1 = 0.06 TLR/mm, 1 = 0.42 total TLR/mm. The assays were repeated at least three times with *N*: 15/genotype. Values were calculated as the number of total TLRP or TLR per the sum of total LR length and normalized with the value of the wild-type (WT) control.
(e) Proposed model for the regulation of secondary and tertiary roots development. All arrows between actors indicate direct regulation (Orosa-Puente *et al.*, 2018). Blue inside the root indicates *AtHB23* expression pattern.

which modulates the three-dimensional shape of the root system. The enhanced density of emerged tertiary roots in *amiR23* plants is consistent with the direct regulatory role of AtHB23 over *LBD16*. AtHB23 represses *LBD16* only during LR initiation from the main root, whereas the expanded expression pattern of *AtHB23* in tertiary roots allows the downregulation of *LBD16* during the initiation, development and emergence of tertiary roots.

DISCUSSION

Main roots and LRs grow in the soil in three dimensions, sensing and uptaking water and micronutrients, and responding to soil biotic and abiotic signals. Methodological limitations led the scientific community to explore the root system of model species mostly in two dimensions, particularly focusing on the formation of secondary roots, rather than on higher-order LRs.

A deep understanding of which genes, pathways, interactions and relationships are involved in root architectural development can impact crop improvement (de Dorlodot *et al.*, 2007). LR formation follows a complex mechanism in which each cell type has specific and determinate roles, under the fine regulation of several TFs and hormones. LRs are mainly differentiated from the primary root due to their post-embryonic origin from the pericycle cell layer of the primary root (Malamy and Benfey, 1997). Other differences in growth have been described; however, the mechanistic basis underlying such distinctions is unclear (Duan *et al.*, 2013). The response to gravity also differs between the primary and LRs (Kiss *et al.*, 2002; Guyomarc'h *et al.*, 2012). In contrast to the immediate response of the primary root to gravity, even before germination (Ma and Hasenstein, 2006), newly emerged LRs in Arabidopsis become gradually more gravitropic over time. These differences have important effects on the final root system architecture and enable the plant to explore larger domains in the soil environment. Differences in the branching capacities of primary and secondary roots remain completely unexplored.

In the model plant Arabidopsis, TFs from several families were duplicated and trebled during evolution and

sometimes seem to be redundant. However, deep studies have demonstrated that each TF has a particular expression pattern and function. For example, ARF ARF19 and ARF7 seem to be involved in the same mechanisms; however, *arf19*- and *arf7*-isolated mutants exhibit auxin-resistant phenotypes and the double-mutant has stronger differential behavior, indicating that both are necessary (Li *et al.*, 2006). Their differential expression patterns indicate that their contributions to auxin signaling in LR development are unique, although each is capable of rescuing the other mutant and they share the same targets (Li *et al.*, 2006). LR initiation and post-initiation events require auxin accumulation (Benková *et al.*, 2003; Péret *et al.*, 2009a), which is produced in the aerial organs (Lijung *et al.*, 2005). Roots are also a source of auxin, but only after LR emergence. For this reason, root-produced auxin has been suggested to not play a role in LR emergence (Lijung *et al.*, 2005).

Many research groups have studied LR development from different points of view and in a variety of plant species; however, several aspects are still poorly understood. In this work, we identified a TF from the HD-Zip I family as an actor in the complex scenario of LR development. We determined that AtHB23 is an auxin-responsive gene expressed in the early stages of LR development and is later restricted to the base of the LRP. The phenotypic characterization of *AtHB23*-silenced (*amiR23*) plants indicated that this TF acts as a negative modulator of LR initiation. Furthermore, we demonstrated that AtHB23 directly represses *LBD16*, a key factor in LR development. In accordance with the link between LBD and HD-Zip I TFs, previous reports indicated that in *M. truncatula*, MtHB1 repressed *MtLBD1* in response to salinity stress. The comparison of these two HD-Zip/LBD relationships highlights common and different critical features: AtHB23 is not the closest Arabidopsis member of MtHB1, which is closely related to the pair AtHB7/12 and, in Medicago, MtHB1 function is related to LR emergence and main root elongation (Ariel *et al.*, 2010a,b), whereas AtHB23 is involved in secondary root initiation, as well as in tertiary root initiation and emergence. Strikingly, AtHB23 turned out to be a direct activator of *LAX3*, suggesting that HD-Zip TFs may act as activators or repressors of transcription, depending on their interacting partners. Based on *in vitro* EMSA assays, it was first proposed that ARF7 and ARF19 directly regulate *LBD16* (Okushima *et al.*, 2007; Lee *et al.*, 2015). The direct regulation of *LBD16* by ARF7 was later demonstrated *in vivo* (Lavenus *et al.*, 2015; Orosa-Puente *et al.*, 2018). LBD16 was previously reported as an inducer of LR formation, along with LBD18 acting downstream of ARF7 and ARF19. This was suggested because double-mutants had less emerged and total LR than did individual *lbd16* and *lbd18* mutants. It was proposed that LBD16 and LBD18 function in the initiation and emergence of LR formation via a different pathway (Lee *et al.*, 2009). Because LR initiation is finely orchestrated by an intricate network of TFs and *AtHB23* exhibits in its promoter putative sequences bound by ARF TFs (TgTCTC), we speculated that AtHB23 may be an additional connector between ARFs and *LBD16* (Figure 7e). However, *AtHB23* was not identified as an ARF7-dependent auxin-responsive gene after 4 h of treatment with 1 μM NAA (Lavenus *et al.*, 2015). Considering that *AtHB23* exhibits a more delayed transcriptional response to auxin (Figure 2a), we assessed *AtHB23* behavior in response to auxin in Col 0 and *arf7/19* seedlings after 12 h with 1 μM IAA. Interestingly, *AtHB23* induction was impaired in the *arf7/19* double-mutants, as was *LBD16* and *LAX3*. Our results indicate that *AtHB23* acts downstream of ARF7, although later than other auxin-responsive genes. This observation agrees with the fact that AtHB23 is a negative regulator of *LBD16* and LR development that likely participates in an auxin-triggered negative feedback loop, thereby fine-tuning LR formation in response to internal and external stimuli, as has been proposed for other auxin-responsive TFs (Gibbs *et al.*, 2014). It was previously shown that *LBD16* is dynamically regulated by ARF7, notably peaking at 10 min of NAA treatment and gradually decreasing afterward (Orosa-Puente *et al.*, 2018). Here, we assessed ARF7 binding with longer IAA treatments, considering the delayed activation of *AtHB23* by auxin. We confirmed by ChIP-qPCR that *AtHB23* is a direct target of ARF7, appearing as a direct molecular link between ARF7 and *LAX3*. In the early stages of LR development, ARF7 activates *LBD29* transcription and LBD29 directly promotes *LAX3* expression only in the surrounding cell layers of young primordia (Figure 7e; Porco *et al.*, 2016). In this work, we showed that *AtHB23* is directly induced by ARF7 later in LR development. Notably, *AtHB23* knockdown impairs *LAX3* promoter activity only in emerged LRs, indicating that alternative TFs regulate the expression of auxin carriers at successive stages of LR development. Strikingly, at 4 h treatment, we still detected ARF recognition of *LBD16* promoter, albeit to a lesser extent compared with *AtHB23*. Remarkably, after 12 h IAA treatment, once *AtHB23* is already induced by exogenous auxin, ARF7 recognition over *LBD16* is already undetectable, whereas the binding to *AtHB23* promoter is partially impaired. Our results support the hypothesis of the ARF-mediated dynamic coordination of TF expression throughout LR development.

LAX3 is normally expressed in cortical and epidermal cells overlying the LR, but not in the primordium itself, and is induced by auxin in the cortex and epidermis (Swarup *et al.*, 2008). This expression pattern was visualized in this work when doing GUS reactions for short times (3 h); however, staining for prolonged periods (overnight) led to a full extended expression to the rest of the primordium (Figures 3 and S7a). The encoded auxin influx transporter

promotes LR emergence by increasing the auxin content of the cortical and epidermal cells directly facing the primordium (Péret *et al.*, 2009b). Here, we show that the AtHB23-dependent response modulates auxin transport by the direct regulation of *LAX3* in the emerged secondary roots.

Interestingly, *LAX3* promoter activity during secondary and tertiary LR formation seems to respond differently to *AtHB23* knockdown. Moreover, *AtHB23* expression patterns also differ between secondary and tertiary root development, likely repressing *LBD16* from expanded regions of TLR primordia. Accordingly, the LR phenotypes that results from *AtHB23* deregulation are different between first- and second-order root branching. Hence, our work on AtHB23 hints that alternative genetic programs regulate the developmental events that lead to the formation of secondary and tertiary roots, thus expanding our understanding of the molecular mechanisms underlying the complexity of the root system. Moreover, the physiological behavior of the primary and secondary roots differ in response to the environment and hormones, such as auxin and ABA (Lijung *et al.*, 2005; Duan *et al.*, 2013). Our findings contribute to the understanding of the molecular mechanisms governing developmental differences between secondary and tertiary root formation.

EXPERIMENTAL PROCEDURES

Plant material, growth conditions, transformation and crosses

For auxin treatments, ChIP assays and root phenotyping, *Arabidopsis thaliana* plants (Col-0 ecotype) were grown in a growth chamber at 22–24°C under long-day conditions (16/8 h light/dark cycles) with a light intensity of approximately 70 μmol m^{-2} sec^{-1} in vertical square Petri dishes (12 × 12 cm) with Murashige–Skoog medium supplemented with vitamins (MS; PhytoTechnology Laboratories, https://phytotechlab.com/home). Seeds were surface sterilized and placed 1 cm from the top for 3 days at 4°C before placing the dishes in the growth chamber.

The lengths of the main root and LRs were measured using the RootNav free software from photographs of the plates (Pound *et al.*, 2013).

The stable transformations of Arabidopsis plants were performed via a floral dip procedure (Clough and Bent, 1998) using *Agrobacterium tumefaciens* strain, LBA4404, carrying the constructs described below. Transformed plants were selected based on their resistance to the appropriate selector chemical (Basta 50 mg L^{-1} or kanamycin 50 mg L^{-1}).

Transgene insertions were verified by PCR using genomic DNA as a template and specific oligonucleotides (Table S1). Three positive independent lines were further reproduced, and homozygous T3 and T4 plants were used for further analyses.

Transgenic plants carrying *AUX/LAX* promoters fused to *GUS* have been previously described (*PromAUX1:GUS*: Marchant *et al.*, 1999, 2002; *PromLAX1:GUS*: Bainbridge *et al.*, 2008; *PromLAX3:GUS*: Swarup *et al.*, 2008). These were generously gifted by Dr Swarup's lab. *DR5:GUS* transgenic plants were obtained from ABRC (Arabidopsis Biological Resource Center).

AmiR23 plants were fertilized with pollen from *PromAUX1:GUS*, *PromLAX1:GUS*, *PromLAX3:GUS* and *DR5:GUS* plants, and then selected by GUS histochemistry.

Genetic constructs

35S::amiR23 and *35S::AtH23* were previously described (Ribone *et al.*, 2015).

PromAtHB23::GUS, a fragment of 1793 bp upstream of the starting codon of *AtHB23*, was amplified from WT genomic DNA and cloned into a *pGEM T-easy* vector, then subcloned into *Bam*HI and *Eco*RI sites in a *pENTR3C* plasmid. Finally, the promoter region was cloned into a *pKGWFS7* vector by GATEWAY recombination.

PromAtHB23:AtHB23:GFP:GUS, the CDS of *AtHB23* (778 bp), was amplified by PCR and cloned in a *pGEM T-easy* vector. Then, it was subcloned between sites *Not*I and *Xho*I in the *pENTR3C* vector carrying *PromAtHB23:GUS* (construct described above). Finally, the entire fragment was cloned in *pKGWFS7* by GATEWAY recombination.

GUS histochemistry

In situ assays of GUS activity were performed essentially as described by Jefferson *et al.* (1987), with a few modifications (Ribone *et al.*, 2015).

RNA isolation and analysis

The total RNA used in quantitative reverse transcriptase RT-qPCR was isolated from Arabidopsis roots using Trizol® reagent (Invitrogen, https://www.thermofisher.com/ar/), according to the manufacturer's instructions. One microgram of RNA was reverse-transcribed using oligo(dT)18 and M-MLV reverse transcriptase II (Promega, https://worldwide.promega.com/). Quantitative real-time PCR (qPCR) was performed using a Mx3000P Multiplex qPCR system (Stratagene, La Jolla, CA, USA, https://agilent.com); each reaction contained a 20 μl final volume that included 2 μl SyBr green (4×), 8 pmol of each primer, 2 mM $MgCl_2$, 10 μl of a 1/15 dilution of the RT reaction and 0.1 μl Taq Platinum (Invitrogen). Fluorescence was measured at 72°C over 40 cycles. Specific primers were designed (Table S1). The quantification of mRNA levels was achieved by normalization against *ACTIN* transcripts levels (*ACTIN2* and *ACTIN8*), following the ΔΔCt method. All reactions were performed with at least three biological replicates and bars represent SEM.

Histology and microscopy

Arabidopsis root sections were harvested and subjected to histochemistry. Then, sections were fixed, dehydrated and imbibed in Histoplast, as previously described (Moreno Piovano *et al.*, 2017). Transverse root sections were mounted on slides and visualized in an Eclipse E200 Microscope (Nikon, Tokyo, Japan, https://www.nikon.com/) equipped with a Nikon Coolpix L810 camera.

Chromatin immunoprecipitation followed by quantitative polymerase chain reaction

For ChIP-qPCR assays, 10-day-old seedlings bearing the construct *PromAtHB23:AtHB23:GFP:GUS* were harvested and nuclei prepared as described in Lucero *et al.* (2017). For ChIP-qPCR assays in which *PromARF7:ARF7:GR* transformed plants were used, 15-day-old seedlings were treated for 4 and 12 h with 1 μM IAA and 2 μM dexamethasone. For the IPs, protein A

Dynabeads (Thermo, https://www.thermofisher.com/ar/) and anti-GFP ab6556 or anti-GR ab3580 antibodies (Abcam) were used. In both ChIP-qPCR experiments, anti-IgG ab6702 antibody (Abcam, https://www.abcam.com/) was used as the negative control. Chromatin was sheared using the Picoruptor sonicator (Diagenode, https://www.diagenode.com/; 10 cycles 30″ ON, 30″ OFF). PCR with specific oligonucleotides (Table S1) was performed using the Sso Advanced Universal mix (BioRad, https://www.bio-rad.com/) in a StepOne device (Applied Biosystems, https://www.thermofisher.com/ar/).

Statistical analysis

The evaluations of primary root length and the number of initiated and emerged secondary roots (shown in Figures 1 and 5, and Figures S3, S4 and S8) were performed using one-way analysis of variance (ANOVA) considering genotype as the main factor. Significant differences (**$P < 0.01$, ***$P < 0.001$, ****$P < 0.0001$) between means were analyzed using *post hoc* Tukey comparison. The data shown in Figures 2, 3, 6 and S5 were analyzed using a two-way ANOVA considering genotype and treatment. When interaction terms were significant ($P < 0.01$), differences between means were analyzed using Tukey comparison and are indicated by different letters. The numbers of biological replicates for each assessment are indicated in the corresponding figures.

ACCESSION NUMBERS

AT1G26960 (AtHB23); AT1G69780 (AtHB13); AT2G42430 (LBD16); AT3G58190 (LBD29); AT2G31310 (LBD14); At1g19220 (ARF19); AT5G20730 (ARF7).

ACKNOWLEDGEMENTS

This work was supported by Agencia Nacional de Promoción Científica y Tecnológica (PICT 2016 0289 to FDA; PICT 2014 3300, PICT 2015 2671 and PICT 2017 0300 to RLC) and CONICET. MFP and PR are CONICET PhD and post-doctoral Fellows, respectively. JVC, FDA and RLC are CONICET Career members. The authors are very grateful to Dr Tom Beeckman for generously sharing *arf7/19* mutants and *PromARF7:ARF7:GR*. The authors thank Dr Ranjan Swarup for kindly providing *aux/lax* single- and quadruple-mutant as well as *AUX/LAX* promoters fused to *GUS* seeds used in this study to our colleague Dr Javier Moreno.

CONFLICT OF INTEREST

The authors declare no competing interests.

AUTHORS' CONTRIBUTION

Conceived and designed the experiments: MFP, FDA and RLC. Performed the experiments: MFP, PAR and JVC. Analyzed the data: MFP, FDA and RLC. Conceived and wrote the paper: FDA and RLC.

SUPPORTING INFORMATION

Additional Supporting Information may be found in the online version of this article.

Figure S1. *AtHB23* expression pattern is different in primary and secondary roots.

Figure S2. Transcription levels of *AtHB23* in *amiR23* and *AT23* roots.

Figure S3. *AtHB23* acts as a repressor of lateral root initiation.

Figure S4. *35S:AtHB23* rescues the differential phenotype of *amiR23* plants.

Figure S5. *AtHB23* silenced plants are less sensitive to auxin.

Figure S6. NPA treatment confirmed that *AtHB23* silenced plants are less sensitive to auxin.

Figure S7. *LAX3* is similarly expressed during secondary and tertiary root development, but differentially depends on AtHB23.

Figure S8. Relative transcript levels of *GFP* in *PromAtHB23:AtHB23:GFP* plants.

Figure S9. Differences in secondary and tertiary roots due to AtHB23 are supported by independent silenced lines.

Table S1. Oligonucleotides used for cloning or qPCR assays.

REFERENCES

Arce, A.L., Raineri, J., Capella, M., Cabello, J.V. and Chan, R.L. (2011) Uncharacterized conserved motifs outside the HD-Zip domain in HD-Zip subfamily I transcription factors; a potential source of functional diversity. *BMC Plant Biol.* **11**, 42.

Ariel, F.D., Manavella, P.A., Dezar, C.A. and Chan, R.L. (2007) The true story of the HD-Zip family. *Trends Plant Sci.* **12**, 419–426.

Ariel, F.D., Diet, A., Verdenaud, M., Gruber, V., Frugier, F., Chan, R.L. and Crespi, M. (2010a) Environmental regulation of lateral root emergence in *Medicago truncatula* requires the HD-Zip I transcription factor HB1. *Plant Cell*, **22**, 2171–2183.

Ariel, F.D., Diet, A., Crespi, M. and Chan, R.L. (2010b) The LOB-like transcription factor MtLBD1 controls *Medicago truncatula* root architecture under salt stress. *Plant Signal. Behav.* **5**, 12.

Bainbridge, K., Guyomarc'h, S., Bayer, E., Swarup, R., Bennett, M., Mandel, T. and Kuhlemeier, C. (2008) Auxin influx carriers stabilize phyllotactic patterning. *Genes Dev.* **22**, 810–823.

Benková, E., Michniewicz, M., Sauer, M., Teichmann, T., Seifertová, D., Jürgens, G. and Friml, J. (2003) Local, efflux-dependent auxin gradients as a common module for plant organ formation. *Cell*, **115**, 591–602.

Berckmans, B., Vassileva, V., Schmid, S.P.C. *et al.* (2011) Auxin-dependent cell cycle reactivation through transcriptional regulation of Arabidopsis E2Fa by lateral organ boundary proteins. *Plant Cell*, **23**, 3671–3683.

Cabello, J.V. and Chan, R.L. (2012) The homologous homeodomain-leucine zipper transcription factors HaHB1 and AtHB13 confer tolerance to drought and salinity stresses via the induction of proteins that stabilize membranes. *Plant Biotechnol. J.* **10**, 815–825.

Calderón Villalobos, L.I.A., Lee, S., De Oliveira, C. *et al.* (2012) A combinatorial TIR1/AFB–Aux/IAA co-receptor system for differential sensing of auxin. *Nat. Chem. Biol.* **8**, 477–485.

Chan, R.L., Gago, G.M., Palena, C.M. and Gonzalez, D.H. (1998) Homeoboxes in plant development. *Biochim. Biophys. Acta*, **1442**, 1–19.

Choi, H., Jeong, S., Kim, D.S., Na, H.J., Ryu, J.S., Lee, S.S., Nam, H.G., Lim, P.O. and Woo, H.R. (2014) The homeodomain-leucine zipper ATHB23, a phytochrome B-interacting protein, is important for phytochrome B-mediated red light signaling. *Physiol. Plant.* **150**, 308–320.

Clough, S.J. and Bent, A.F. (1998) Floral dip: a simplified method for Agrobacterium-mediated transformation of *Arabidopsis thaliana*. *Plant J.* **16**, 735–743.

De Smet, I., Tetsumura, T., De Rybel, B. *et al.* (2007) Auxin-dependent regulation of lateral root positioning in the basal meristem of Arabidopsis. *Development*, **134**, 681–690.

de Dorlodot, S., Forster, B., Pagès, L., Price, A., Tuberosa, R. and Draye, X. (2007) Root system architecture: opportunities and constraints for genetic improvement of crops. *Trends Plant Sci.* **12**, 474–481.

Duan, L., Dietrich, D., Ng, C.H., Chan, P.M.Y., Bhalerao, R., Bennett, M.J. and Dinnen, J.R. (2013) Endodermal ABA signaling promotes lateral root quiescence during salt stress in Arabidopsis seedlings. *Plant Cell*, **25**, 324–334.

Friml, J., Vieten, A., Sauer, M., Weijers, D., Schwarz, H., Hamann, T., Offringa, R. and Jürgens, G. (2003) Efflux-dependent auxin gradients establish the apical-basal axis of Arabidopsis. *Nature*, **426**, 147–153.

Gao, D., Appiano, M., Huibers, R.P., Chen, X., Loonen, A.E.H.M., Visser, R.G.F., Wolters, A.M.A. and Bai, Y. (2014) Activation tagging of ATHB13

in *Arabidopsis thaliana* confers broad-spectrum disease resistance. *Plant Mol. Biol.* **86**, 641–653.

Gehring, W.J. (1987) Homeoboxes in the study of development. *Science*, **236**, 1245–1252.

Gibbs, D.J., Voß, U., Harding, S.A. *et al.* (2014) AtMYB93 is a novel negative regulator of lateral root development in Arabidopsis. *New Phytol.* **203**, 1194–1207.

Goh, T., Joi, S., Mimura, T. and Fukaki, H. (2012) The establishment of asymmetry in Arabidopsis lateral root founder cells is regulated by LBD16/ASL18 and related LBD/ASL proteins. *Development*, **139**, 883–893.

Guyomarc'h, S., Léran, S., Auzon-Cape, M., Perrine-Walker, F., Lucas, M. and Laplaze, L. (2012) Early development and gravitropic response of lateral roots in *Arabidopsis thaliana*. *Philos. Trans. R. Soc. Lond. B Biol. Sci.* **367**, 1509–1516.

Hanson, J., Johannesson, H. and Engström, P. (2001) Sugar-dependent alterations in cotyledon and leaf development in transgenic plants expressing the HDZip gene ATHB13. *Plant Mol. Biol.* **45**, 247–262.

Hanson, J., Regan, S. and Engström, P. (2002) The expression pattern of the homeobox gene ATHB13 reveals a conservation of transcriptional regulatory mechanisms between Arabidopsis and hybrid aspen. *Plant Cell Rep.* **21**, 81–89.

Henriksson, E., Olsson, A.S., Johannesson, H., Johansson, H., Hanson, J., Engström, P. and Söderman, E. (2005) Homeodomain leucine zipper class I genes in Arabidopsis. Expression patterns and phylogenetic relationships. *Plant Physiol.* **139**, 509–518.

Jefferson, R.A., Kavanagh, T.A. and Bevan, M.W. (1987) GUS fusions: beta-glucuronidase as a sensitive and versatile gene fusion marker in higher plants. *EMBO J.* **6**, 3901–3907.

Jeon, E., Young Kang, N., Cho, C., Joon Seo, P., Chung Suh, M. and Kim, J. (2017) LBD14/ASL17 positively regulates lateral root formation and is involved in ABA response for root architecture in Arabidopsis. *Plant Cell Physiol.* **58**, 2190–2201.

Johannesson, H., Wang, Y. and Engström, P. (2001) DNA-binding and dimerization preferences of Arabidopsis homeodomain–leucine zipper transcription factors in vitro. *Plant Mol. Biol.* **45**, 63–73.

Kim, Y.K., Son, O., Kim, M.R., Nam, K.H., Kim, G.T., Lee, M.S., Choi, S.Y. and Cheon, C.I. (2007) ATHB23, an Arabidopsis class I homeodomain-leucine zipper gene, is expressed in the adaxial region of young leaves. *Plant Cell Rep.* **26**, 1179–1185.

Kiss, J.Z., Miller, K.M., Ogden, L.A. and Roth, K.K. (2002) Phototropism and gravitropism in lateral roots of Arabidopsis. *Plant Cell Physiol.* **43**, 35–43.

Kumpf, R.P., Shi, C.L., Larrieu, A., Stø, I.M., Butenko, M.A., Péret, B., Riiser, E.S., Bennett, M.J. and Aalen, R.B. (2013) Floral organ abscission peptide IDA and its HAE/HSL2 receptors control cell separation during lateral root emergence. *Proc. Natl Acad. Sci. USA*, **110**, 5235–5240.

Lavenus, J., Goh, T., Roberts, I., Guyomarc'h, S., Lucas, M., De Smet, I., Fukaki, H., Beeckman, T., Bennett, M. and Laplaze, L. (2013) Lateral root development in Arabidopsis: fifty shades of auxin. *Trends Plant Sci.* **18**, 450–458.

Lavenus, J., Tatsuaki Goh, T., Guyomarc'h, S. *et al.* (2015) Inference of the Arabidopsis lateral root gene regulatory network suggests a bifurcation mechanism that defines primordia flanking and central zones. *Plant Cell*, **27**, 1368–1388.

Lee, H.W., Kim, N.Y., Lee, D.J. and Kim, J. (2009) LBD18/ASL20 regulates lateral root formation in combination with LBD16/ASL18 downstream of ARF7 and ARF19 in Arabidopsis. *Plant Physiol.* **151**, 1377–1389.

Lee, H.W., Kim, M.J., Kim, N.Y., Lee, S.H. and Kim, J. (2012) LBD18 acts as a transcriptional activator that directly binds to the EXPANSIN14 promoter in promoting lateral root emergence of Arabidopsis. *Plant J.* **73**, 212–224.

Lee, H.W., Cho, C. and Kim, J. (2015) Lateral organ boundaries domain16 and 18 act downstream of the AUXIN1 and LIKE-AUXIN3 auxin influx carriers to control lateral root development in Arabidopsis. *Plant Physiol.* **168**, 1792–1806.

Li, J., Dai, X. and Zhao, Y. (2006) A role for auxin response factor 19 in auxin and ethylene signaling in Arabidopsis. *Plant Physiol.* **140**, 899–908.

Lijung, K., Hull, A.K., Celenza, J., Yamada, M., Estelle, M., Normanly, J. and Sandberg, G. (2005) Sites and regulation of auxin biosynthesis in Arabidopsis roots. *Plant Cell*, **17**, 1090–1104.

Lucas, M., Guédon, Y., Jay-Allemand, C., Godin, C. and Laplaze, L. (2008) An auxin transport-based model of root branching in *Arabidopsis thaliana*. *PLoS One*, **3**, e3673.

Lucero, L.E., Manavella, P.A., Gras, D.E., Ariel, F.D. and Gonzalez, D.H. (2017) Class I and class II TCP transcription factors modulate SOC1-dependent flowering at multiple levels. *Mol. Plant*, **10**, 1571–1574.

Ma, Z. and Hasenstein, K.H. (2006) The onset of gravisensitivity in the embryonic root of flax. *Plant Physiol.* **140**, 159–166.

Malamy, J.E. and Benfey, P.N. (1997) Organization and cell differentiation in lateral roots of *Arabidopsis thaliana*. *Development*, **124**, 33–44.

Marchant, A., Kargul, J., May, S.T., Muller, P., Delbarre, A., Perrot-Rechenmann, C. and Bennett, M.J. (1999) AUX1 regulates root gravitropism in Arabidopsis by facilitating auxin uptake within root apical tissues. *EMBO J.* **18**, 2066–2073.

Marchant, A., Bhalerao, R., Casimiro, I., Eklöf, J., Casero, P.J., Bennett, M. and Sandberg, G. (2002) AUX1 promotes lateral root formation by facilitating indole-3-acetic acid distribution between sink and source tissues in the Arabidopsis seedling. *Plant Cell*, **14**, 589–597.

Moreno Piovano, G.S., Moreno, J.E., Cabello, J.V., Arce, A.L., Otegui, M.E. and Chan, R.L. (2017) A role for LAX2 in regulating xylem development and lateral-vein symmetry in the leaf is uncovered by studying transgenic plants expressing HaHB4, a sunflower transcription factor. *Ann. Bot.* **120**, 577–590.

Motte, H. and Beeckman, T. (2019) The evolution of root branching: increasing the level of plasticity. *J. Exp. Bot.* **70**, 785–793.

Okushima, Y., Fukaki, H., Onoda, M., Theologis, A. and Tasaka, M. (2007) ARF7 and ARF19 regulate lateral root formation via direct activation of LBD/ASL genes in Arabidopsis. *Plant Cell*, **19**, 118–130.

Orosa-Puente, B., Leftley, N., von Wangenheim, D. *et al.* (2018) Root branching toward water involves posttranslational modification of transcription factor ARF7. *Science*, **362**, 1407–1410.

Osmont, K.S., Sibout, R. and Hardtke, C.S. (2007) Hidden branches: developments in root system architecture. *Annu. Rev. Plant Biol.* **58**, 93–113.

Palena, C.M., Gonzalez, D.H. and Chan, R.L. (1999) A monomer-dimer equilibrium modulates the interaction of the sunflower homeodomain-leucine zipper protein HAHB-4 with DNA. *Biochem. J.* **341**, 81–87.

Péret, B., de Rybel, B., Casimiro, I., Benkova, I., Swarup, R., Laplaze, L., Beeckman, T. and Bennett, M.J. (2009a) Arabidopsis lateral root development: an emerging story. *Trends Plant Sci.* **14**, 399–408.

Péret, B., Larrieu, A. and Bennett, M.J. (2009b) Lateral root emergence: a difficult birth. *J. Exp. Bot.* **60**, 3637–3643.

Péret, B., Swarup, K., Ferguson, A. *et al.* (2012) AUX/LAX genes encode a family of auxin influx transporters that perform distinct functions during Arabidopsis development. *Plant Cell*, **24**, 2874–2885.

Perotti, M.F., Ribone, P.A. and Chan, R.L. (2017) Plant transcription factors from the Homeodomain-Leucine Zipper family I. Role in development and stress responses. *IUBMB Life*, **69**, 280–289.

Porco, S., Larrieu, A., Du, Y. *et al.* (2016) Lateral root emergence in Arabidopsis is dependent on transcription factor LBD29 regulation of auxin influx carrier LAX3. *Development*, **143**, 3340–3349.

Pound, M.P., French, A.P., Atkinson, J.A., Wells, D.M., Bennett, M.J. and Pridmore, T. (2013) RootNav: navigating images of complex root architectures. *Plant Physiol.* **162**, 1802–1814.

Ribone, P.A., Capella, M. and Chan, R.L. (2015) Functional characterization of the homeodomain leucine zipper I transcription factor AtHB13 reveals a crucial role in Arabidopsis development. *J. Exp. Bot.* **66**, 5929–5943.

Silva, A.T., Ribone, P.A., Chan, R.L., Ligterink, W. and Hilhorst, H.W.M. (2016) A predictive co-expression network identifies novel genes controlling the seed-to-seedling phase transition in *Arabidopsis thaliana*. *Plant Physiol.* **170**, 2218–2231.

Swarup, R. and Péret, B. (2012) AUX/LAX family of auxin influx carriers-an overview. *Front Plant Sci.* **3**, 225.

Swarup, K., Benková, E., Swarup, R. *et al.* (2008) The auxin influx carrier LAX3 promotes lateral root emergence. *Nat. Cell Biol.* **10**, 946–954.

Teale, W. and Palme, K. (2018) Naphthylphthalamic acid and the mechanism of polar auxin transport. *J. Exp. Bot.* **69**, 303–312.

Ulmasov, T., Hagen, G. and Guilfoyle, T.J. (1997) ARF1, a transcription factor that binds to auxin response elements. *Science*, **276**, 1865–1868.

